In situ NMR investigations into the ADMET-reaction of 1,4-diheptyloxy-2,5-divinylbenzene via a Schrock-type molybdenum alkylidene complex

Ralf M. Peetz [a,1], Volker Sinnwell [b], Emma Thorn-Csányi [a,*]

[a] *Institute of Technical and Macromolecular Chemistry, University of Hamburg, Bundesstr. 45, 20146 Hamburg, Germany*
[b] *Institute for Organic Chemistry, University of Hamburg, Martin-Luther-King-Pl. 6, 20146 Hamburg, Germany*

Available online 5 May 2006

Dedicated to Richard R. Schrock

Abstract

The acyclic diene metathesis (ADMET) polycondensation of 1,4-diheptyloxy-2,5-divinylbenzene (DHepODVB) with the Schrock-type alkylidene complex $Mo(NAr^{Me_2})(CHCMe_2Ph)[OCMe(CF_3)_2]_2$ was investigated by means of in situ $^1H/^{13}C$ NMR spectroscopy. Efforts were made to gain insight into the reaction mechanism and explain the relatively high reaction temperatures (>60 °C instead of room temperature in the case of the diheptylsubstituted analog) necessary to achieve useful reaction rates. Different reaction charges were investigated in dependence on reaction time and ratio catalyst/monomer. At least four novel alkylidene species were detected of which three species could be assigned to structures (two of which are binuclear, presumably due to the nearly stoichiometric ratios catalyst/monomer). These three structures show a Mo-coordination from the oxygen of a heptyloxy side chain from the substrate resulting in stabilized intermediates. These intermediates act as low energy "traps" that make the higher reaction temperatures necessary. The stabilization also seems to effect decomposition of active species, substantially slowing it down. Even after 24 days, alkylidene signals could be detected without noticeable reduction in relative amount.
© 2006 Elsevier B.V. All rights reserved.

Keywords: Schrock-type catalysts; Olefin metathesis; ADMET; Molybdenum alkylidene complex; Reaction mechanism

1. Introduction

Olefin metathesis has become a valuable catalysis tool in the synthesis of polymers and otherwise hardly accessible lower molecular weight organic compounds [1–6]. We reported on the acyclic diene metathesis (ADMET) polycondensation of *ring*-substituted *p*-divinylbenzenes [7–11]. The products yielded are soluble mono- or 2,5-disubstituted *p*-phenylene vinylene (PV) oligomers, with all *trans* configuration and defect-free microstructure. The oligomers are suitable for use in highly advanced optical and electronic applications (e.g., OLEDs) [12]. The objective of this contribution is to provide an insight into the mechanism of the ADMET polycondensation reaction of

1,4-diheptyloxy-2,5-divinylbenzene (DHepODVB) illustrated in Scheme 1.

The products are polydisperse oligomers of 2,5-diheptyloxy-*p*-phenylene vinylene (DHepO-PV). These oligomer mixtures are readily separated into fractions of single oligomers [10]. The monodisperse oligomers are valuable materials for optoelectronical applications as well as model substances for the corresponding polymer. The catalyst used is the Schrock-type alkylidene complex $Mo(NAr^{Me_2})(CHCMe_2Ph)$ $[OCMe(CF_3)_2]_2$ ($[Mo]=CH(CH_3)_2Ph$, **A**) depicted in Scheme 2.

Based on investigations in our group regarding structure/reactivity relationships of several Schrock-type tungsten and molybdenum alkylidene complexes [13,14], this molybdenum complex has been shown to be the most active catalyst for the ADMET of substituted divinylbenzenes.

The initiation step and first catalytic cycle for the ADMET condensation of DHepODVB with the alkylidene complex are sketched in Scheme 3.
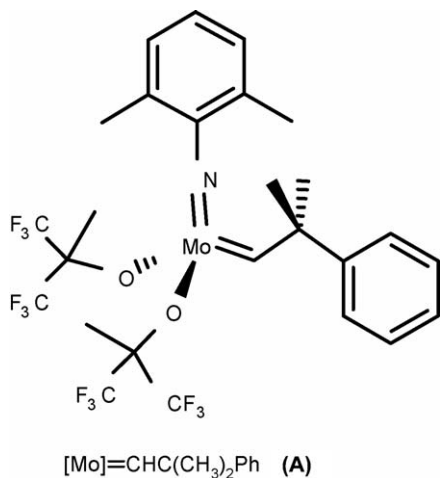
* Corresponding author. Tel.: +49 40 42838 3166; fax: +49 40 42838 6008.
E-mail address: thorn@uni-hamburg.de (E. Thorn-Csányi).
[1] Present address: Center for Engineered Polymeric Materials (CePM), City University of New York/College of Staten Island, 2800 Victory Boulevard, Staten Island, NY 10314, United States.
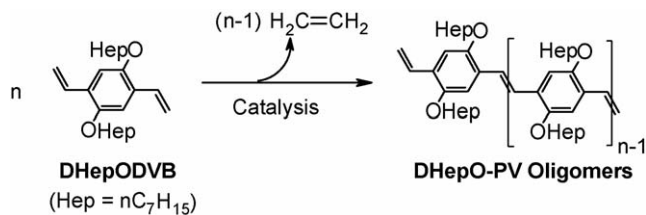
Scheme 1. ADMET condensation of DHepODVB.

Scheme 2. Schrock-type alkylidene Mo(NArMe2)(CHCMe2Ph) [OCMe(CF3)2]2.
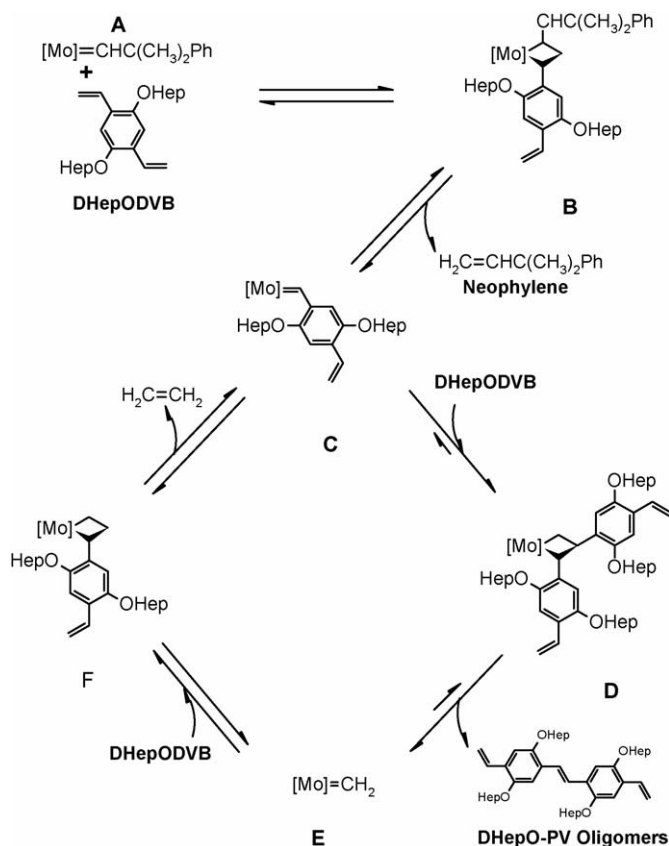
Scheme 3. ADMET of DHepODVB: transalkylidenation/initiation of catalyst and first catalytic cycle (first condensation yields DHepO-PV dimer).

The molybdenum species are marked **A** to **F**. In the initiating step, the alkylidene complex **A** reacts with DHepODVB via a [2 + 2] cycloaddition to form a molybdenacyclobutane species **B**. **B** decomposes productively into a new alkylidene species **C** and neophylene. Now the catalytic cycle starts by **C** adding DHepODVB in another [2 + 2] cycloaddition to form the molybdenacyclobutane species **D**. **D** decomposes productively to a highly reactive methylidene complex **E** and the first condensation product (DHepO-PV oligomer), a dimer. The formation of the sterically highly unfavorable **D** is only possible by arranging the voluminous side chain substituted *p*-styryl units in anti positions regarding the molybdenacyclobutane ring. The formation of the thermodynamically favorable *trans*-vinylene bond in the DHepO-PV oligomers drives this step of the reaction, thus providing a substantial contribution to the overall driving force of the condensation process. **E** quickly reacts with new DHepODVB and forms **F**, which then decomposes to **C** under loss of ethylene. A reverse reaction, i.e., the addition of ethylene to **C** (or theoretically even **E**), is disfavored because ethylene is removed from the equilibrium by applying vacuum to the system under standard reaction conditions. The removal of ethylene is a determining factor for the course of the polycondensation process.

While the ADMET condensation of DHepODVB proceeds, the amount of DHepO-PV dimer will increase. If the concentration of dimer is sufficiently high, it competes with the monomer in the condensation reaction to form higher condensation products (like trimer and tetramer). Consequently, depending on the overall progress of the condensation reaction, the nature of **C**, **D** and **F** will change accordingly.

Comparing the condensation behavior of 1,4-**diheptyl**-2,5-divinylbenzene (DHepDVB) [14] with that of 1,4-**diheptyloxy**-2,5-divinylbenzene under similar experimental conditions, we found substantial differences: After 24 h at 23 °C the reaction with DHepDVB using toluene as solvent yielded oligomers with more than 10 repeat units, whereas DHepODVB gave essentially only trace amounts of dimer (indicated by a slight color change of the solution). In the latter case, reaction temperatures higher than ~60 °C were necessary to achieve satisfying conversions within 24 h. We hypothesized that the oxygen of a side chain was being complexed at the catalyst center, thus causing a stabilization of intermediate species resulting in lower reaction rates [8,10]. Possible species are illustrated in Scheme 4 and show energetically favorable five-membered rings.

To elucidate the ADMET condensation behavior of DHepODVB and find possible proof for these assumptions, we carried out a series of NMR investigations on active condensation mixtures.

2. Results and discussion

In a previous paper we reported on NMR investigations into the ADMET condensation of DHepDVB (see Section 1) and presented the first observation of a molybdenacyclobutane species during a metathesis reaction [14]. In these investigations no active species could be detected after 24 h reaction at room temperature. Decomposition of highly active methylidene species
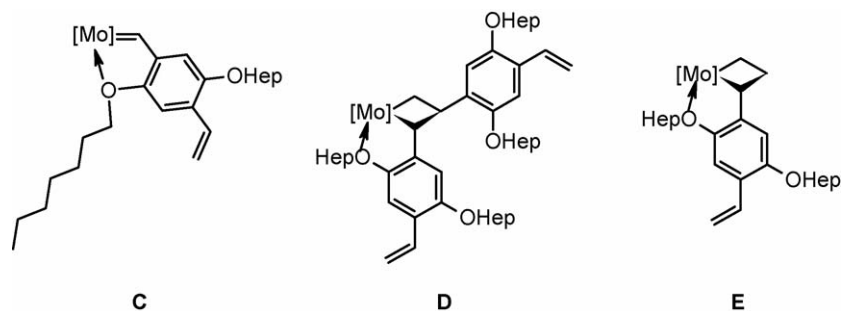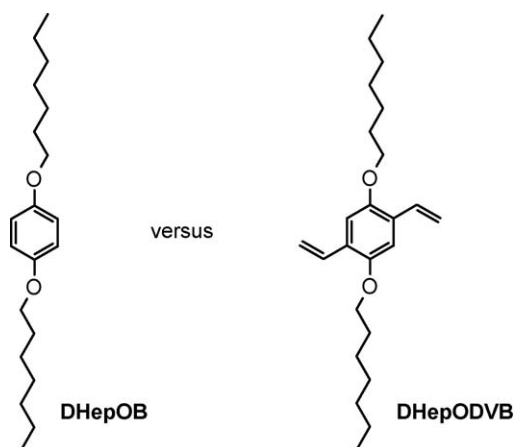
Scheme 4. Possible stabilized intermediates via O-coordination.

such as **E** is speculated to be the most important decomposition process in metathesis reactions [15]. In comparison to the DHepDVB case investigations using DHepODVB showed substantially longer catalyst reactivity: even at reaction temperatures of ~80 °C the catalyst remained active for several hours, even days. We will show data indicating the presence of active species after 24 days (reaction at room temperature). This has to be attributed to the presence of the Lewis basic oxygen in the heptyloxy side chains, causing stabilization of intermediate species (see Section 1).

2.1. Experiments with 1,4-diheptyloxybenzene (DHepOB)

To estimate the isolated contribution of oxygen without the reactive vinyl bonds of DHepODVB present, we investigated the complexation behavior of the structurally similar 1,4-diheptyloxybenzene (Scheme 5).

In a typical experiment, five equivalents of 1,4-diheptyloxybenzene (solution in toluene-d_8) were layered on a frozen catalyst solution in toluene-d_8 in an NMR tube under inert conditions. After the entire content was frozen, the tube was sealed under vacuum. The influence of concentration was investigated semi-quantitatively: because the DHepOB solution was layered on the catalyst solution the rotation of the sample in the NMR spectrometer resulted only in partial mixing. Thus, initial NMR spectra of the reaction mixture acquired during the phase of warming-up to room temperature and thereafter showed an average ratio **A**/DHepOB > 1/5 (e.g.,

A/DHepOB ~ 1/1, see spectra "0 min" and "12.5 min" in Fig. 1 (compare relative intensities of signals from catalyst **A** at 12.18 ppm (1H) or 6.7–7.15 ppm (8H) with those of signals from DHepOB at 3.6–3.8 ppm (4H) and signal at 6.85 ppm (4H)). The reaction charge was then cooled down to ~−90 to −95 °C, thoroughly mixed and investigated again by NMR spectroscopy during warm up to room temperature and at room temperature. Fig. 1 illustrates representative NMR spectra obtained during this experiment, together with a spectrum of isolated **A**.

In the spectra of the reaction mixtures **A**/DHepOB, the chemical shifts of the peaks originating from **A** do not
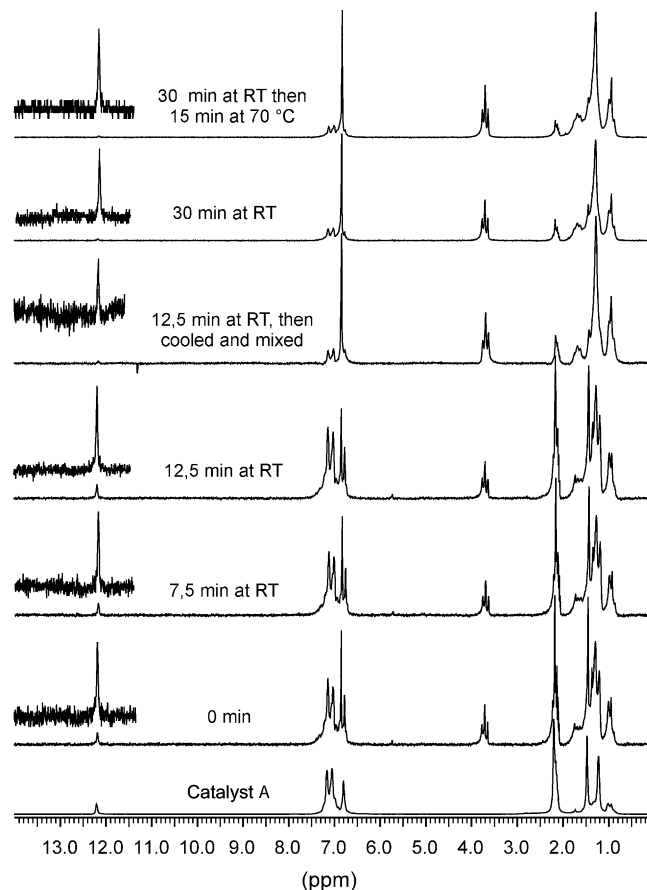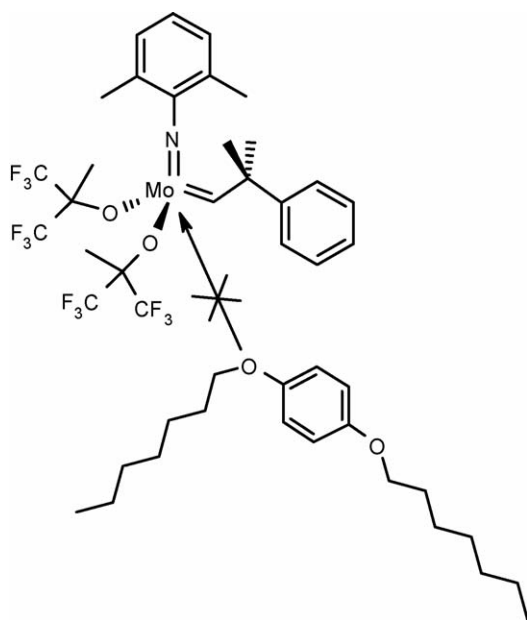

Scheme 5. Structures of DHepOB and DHepODVB.

Fig. 1. ¹H NMR spectra of **A**, and mixture **A** + DHepOB after different reaction times (100 MHz, toluene-d_8; spectra 2–4, **A**/DHepOB ~ 1; spectra 5–7, **A**/DHepOB ~ 1/5).

Scheme 6. Hindered coordination of DHepOB into [Mo] = CHCMe₂Ph.

Fig. 2. ^{1}H NMR spectra of **A**, DHepODVB, and ADMET condensation mixtures **A**/DHepODVB at different reaction times (100 MHz, toluene-d$_8$; mixtures: **A**/DHepODVB = 1/5, [1] = 10 mM, reaction at room temperature under exclusion of light; "0 min" denotes the first spectrum taken of the reaction mixture while heating up from ~−95 °C to room temperature, other spectra at room temperature; insets: enlarged "alkylidene signals".

change significantly (i.e., neither at **A**/DHepOB ~ 1/1, nor at **A**/DHepOB ~ 1/5). Spectra recorded after ~1 h reaction time (not shown) did not show any change either. Obviously, the interaction of the oxygen from the side chains with the metal center does not occur, it is sterically hindered (Scheme 6).

As a consequence, we can assume that the substrate DHepODVB will not approach the Mo-alkylidene complex (via NCO plane) [15] as the result of an interaction of oxygen but rather via the interaction with one vinyl bond. Therefore, mono adducts between DHepODVB and **A** via oxygen are improbable.

2.2. Investigations with 1,4-diheptyloxy-2,5-divinylbenzene

2.2.1. Reaction time dependent NMR spectra

If the oxygen of the free substrate DHepOB does not coordinate into the metal center then we can assume that the oxygen from the free DHepODVB is even less likely to coordinate into the metal center, unless a cooperative chelating effect of oxygen together with one vinyl bond were possible. Intramolecular oxygen coordination of active species should result in stabilized structures (see Section 1). In order to gain insight into these possible structures, we investigated the reaction of DHepODVB with **A** under different reaction conditions by means of ^{1}H NMR spectroscopy.

Reactions were performed in toluene-d$_8$ at room temperature with molar ratios of catalyst A/monomer DHepODVB = 1/1, 1/3 and 1/5 under exclusion of light. The catalyst concentration [**A**] was similar to concentrations used for preparative ADMET condensations [10]. The low **A**/DHepODVB ratios we chose increase the relative concentration of active species in the spectra.

In a typical experiment monomer (solution in toluene-d$_8$) was layered onto a catalyst solution in toluene-d$_8$ at temperatures ~−90 to −95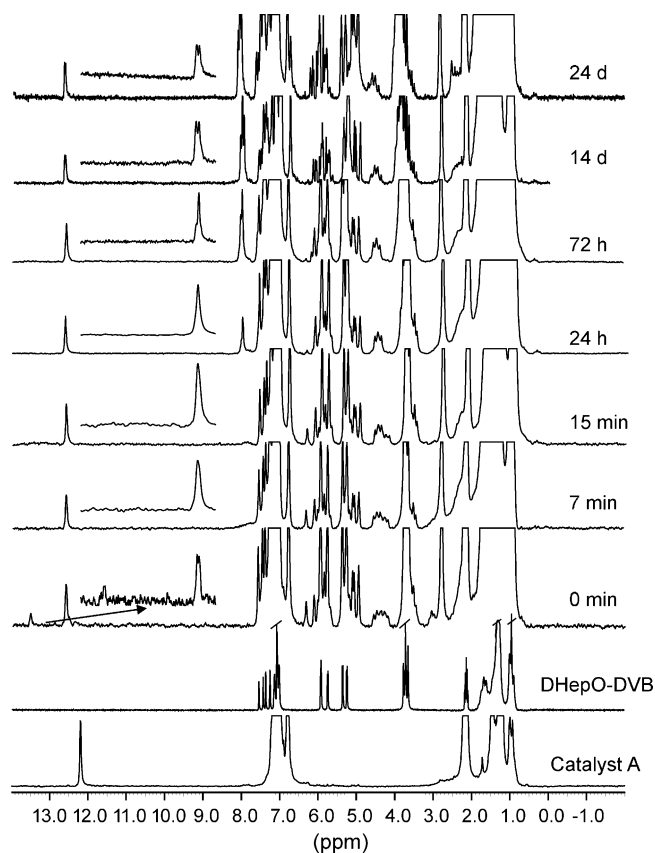 °C in a NMR test tube. The charge was completely frozen in liquid nitrogen, and the tube sealed under vacuum. The first NMR spectrum was then recorded during the warming-up to room temperature (e.g., spectrum "0 min" in Fig. 2) and served as a reference point for the reaction time. During this warming-up period mixing of the catalyst and monomer solutions would occur. All other NMR spectra were recorded at room temperature. During the entire time of the experiment, the tube was covered to prevent possible decompositions caused by light.

Fig. 2 exemplarily shows ^{1}H NMR spectra of an experiment with a charge **A**/DHepODVB ~ 1/5, together with respective spectra of isolated **A** and DHepODVB.

Comparing the spectra of the reaction mixture to those of the isolated catalyst and monomer, several significant differences are observed.

In the $\delta \sim 12$–14 ppm region signals of different alkylidene species can be found (i.e., resonances of protons on an alkylidene carbon **A**, see Scheme 7). In this region, the spectrum at "0 min" shows three resonances at $\delta \sim 13.6$, 12.56 and 12.59 ppm. With progressing reaction time one peak disappears ($\delta \sim 13.6$) and in the region 12.56–12.59 ppm the resolution exists no longer. After 3 days reaction time a second peak is visible at slightly larger chemical shifts, the intensity of which increases in the following spectra. The spectra recorded after 14 and 24 days
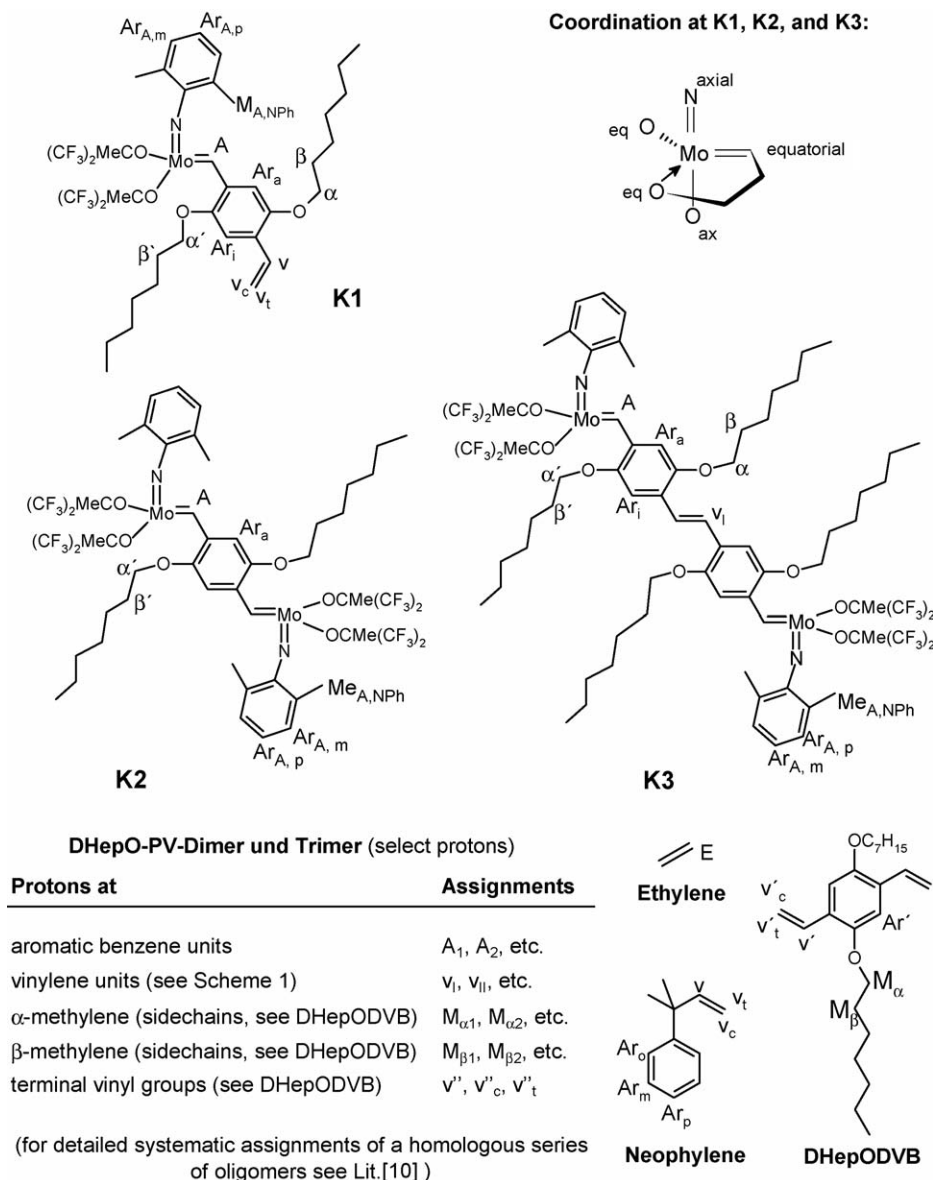
Scheme 7. Identified species (with assignments) in ADMET condensation of DHepODVB using catalyst **A**.

("14 d" and "24 d") do not show significant differences in the alkylidene region.

In the spectra from 24 h upwards, the proton spectra of the reaction mixture show signal intensities at $\delta \sim 2.8, 3.5, 4.2–5.2$ and 6–6.3 ppm which cannot be observed in the spectra of the isolated catalyst or monomer. In the spectrum "24 h" the evolving signal intensity around $\delta \sim 8$ ppm demonstrates the formation of vinylene bonds, indicative of condensation products, DHepO-PV oligomers (for details see below: Fig. 3 and corresponding text), allowing to monitor the reaction progress easily via these product specific signals.

2.2.2. Determination of active species

Using a catalyst (A): DHepODVB ratio of 1:3, ^{1}H and ^{13}C NMR in situ measurements were carried out. These NMR experiments were performed at 23 days reaction time within a time frame of 48 h and included the following: determination of

H–H couplings (COSY), the number of protons per C (DEPT), $^1J_{\text{H–C}}$ coupled C atoms (HMQC), $^2J_{\text{H–C}}/^3J_{\text{H–C}}$ coupled C atoms (HMBC) and H–H coupling due to the NOE.

Scheme 7 illustrates and assigns all structures that were identified in the charge.

Tables 1–3 summarize results from the NMR experiments.

Columns 1–3 list the assignment of the respective proton, their chemical shifts, and their relative intensity. Column 4 presents the chemical shifts of other protons with which the respective proton is experiencing a NOE. Column 5 shows the chemical shifts of the C-atoms to which the respective protons are attached (determined via $^1J_{\text{H–C}}$ coupling), and column 6 lists the chemical shifts of C-atoms with which the respective proton is experiencing either a $^2J_{\text{H–C}}$ or $^3J_{\text{H–C}}$ coupling, thus determining which signals belong to a specific molecule. If a coupling/shift is not given in the tables, it does not mean it was not observed, but rather that the spectral resolution did not suf-
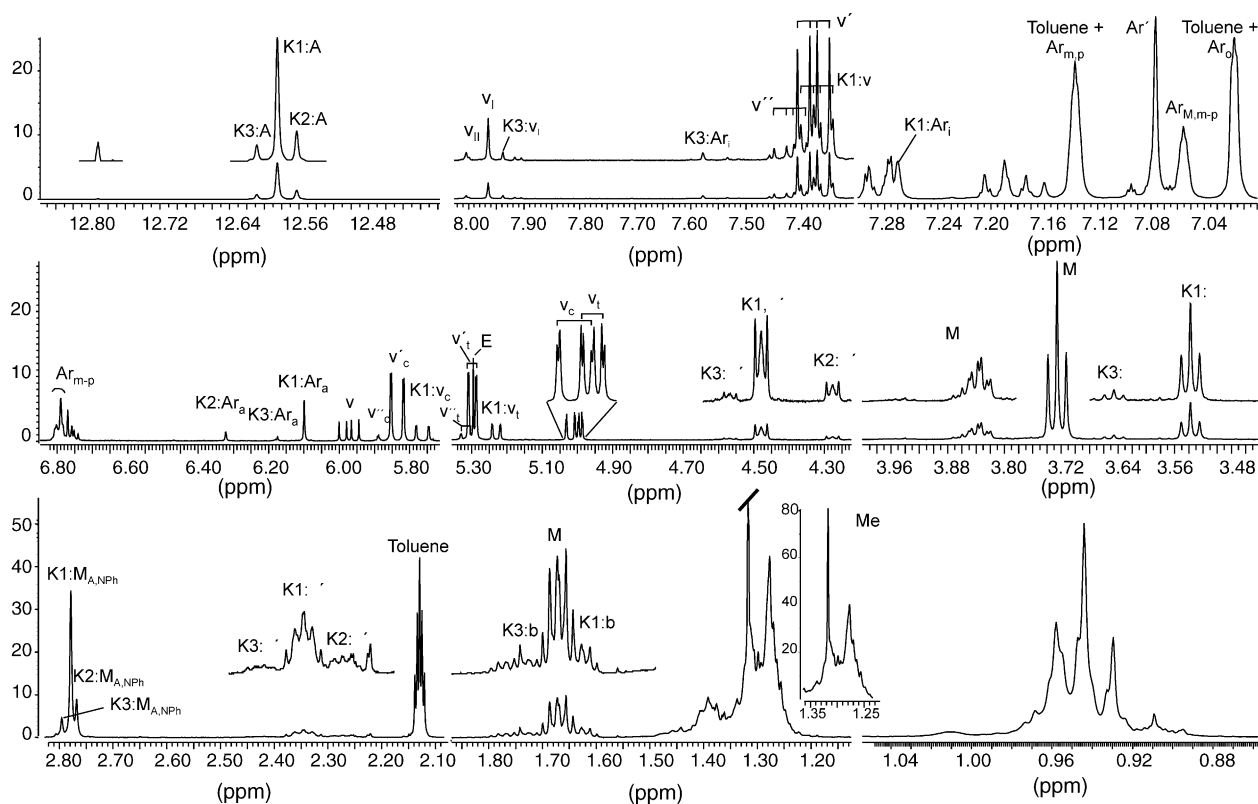
Fig. 3. ^{1}H NMR spectrum of ADMET condensation charge with assignments (500 MHz, toluene-d$_8$; ca. 3 weeks reaction time [**A**] = 10 mM, **A**/DHepODVB ∼ 1/3; spectrum is segmented – regions without signal intensity omitted, specific scaling for each segment; insets: signals with increased vertical scaling).

Table 1
Species **K1**: results from NMR experiments

Proton	δ_H (ppm)	Relative intensity	NOE with H(δ_H (ppm))	$^1J_{H–C}$ mit C(δ_C (ppm))	Relevant $^2J_{H–C}/^3J_{H–C}$ with C(δ_C (ppm))
A	12.59	1	1.3, 2.78, 6.1	n.a.	106, 152, 137
v	dd 7.37	n.r.	n.r.	131	n.r.
Ar$_a$	6.1	1	1.3, 1.63, 2.78, 3.54, 12.59	106	(37), 126, 151, 152
Ar$_i$	s 7.27	∼1	1.3, 2.34, 4.49, 5.765	107	(42), 126, 133, 151, 152
Ar$_{m-p}$	6.79–6.8	3	2.78	127.5	19
v$_c$	dd 5.765	1	7.27, 5.23	125	n.r.
v$_t$	dd 5.23	1	5.765		n.r.
α′	m 4.49	2	1.3, 2.34, 7.27	72	26, 27.5, 151
β′	m 2.34	2	1.3, 1.4, 4.49	27.5	26, 72
α	t 3.54	2	∼1.25–1.4, 1.63	69	27, 30.5, 152
β	m 1.63	n.r.	∼1.25–1.4, 3.54	30.5	n.r.
Me$_{A,NPh}$	s 2.78	6	1.3, 6.79–6.8, 12.59	19	128, 137, 154
MeRF$_6$	1.3	n.r.	n.r.	28	n.r.

Table 2
Species **K2**: results from NMR experiments

Proton	δ_H (ppm)	Relative intensity	NOE with H (δ_H (ppm))	$^1J_{H–C}$ mit C(δ_C (ppm))	Relevant $^2J_{H–C}/^3J_{H–C}$ with C(δ_C (ppm))
A	12.56	1	∼1.25, 2.77, 6.32	n.a.	103, 152.5
Ar$_{m-p}$	6.7–6.8	n.r.	n.r.	127.5	19
Ar$_a$	s 6.32	1	2.28, 4.28, 12.56	103	133, 152.5
α′	m 4.28	2	∼1.25, 2.28, 6.32	72	n.r.
β′	m 2.28	n.r.	n.r.	27	n.r.
Me$_{A,NPh}$	s 2.765	6	6.8	19	n.r.
MeRF$_6$	∼1.25	n.r.	n.r.	n.r.	n.r.

Table 3
Species **K3**: results from NMR experiments

Proton[a]	δ_H (ppm)	Relative intensity	NOE mit H (δ_H (ppm))	$^1J_{H-C}$ mit C (δ_C (ppm))	Relevent $^2J_{H-C}/^3J_{H-C}$ mit C (δ_C (ppm))
A	12.61	1	6.17, 2.80, ~1.31	n.a.	153
v_I	7.94	~1	7.58	124	124
Ar_i	7.58	~1	4.57, 7.94	n.r.	152, 153
Ar_a	6.17	~1	3.65, 2.8	n.r.	152, 153, 127, (37)
α'	4.57	~2	7.58	72	n.r.
β'	2.42	n.r.	n.r.	n.r.	n.r.
α	3.65	~2	6.17, 1.75	69	27, 31
β	1.75	n.r.	3.65	31	n.r.
$Me_{A,NPh}$	2.80	~6	6.8, 12.61	19	n.r.

n.a., not applicable; n.r., not resolved.

[a] **K3** is only present in relatively small concentrations, so less resonances are resolved.

fice. In addition, C–H couplings of carbons with $\delta > 200$ ppm could not be observed due to the spectral width of the experiments.

Fig. 3 details the corresponding assignments of resonances in the ^{1}H NMR spectrum.

Different regions of the spectrum have been expanded and/or enlarged. The relative signal intensities are indicated by the vertical scales for each region. The analysis of this spectrum yields significant observations.

First, there is clear indication for the presence of at least four resonances resulting from alkylidene protons of which three signals were assigned to structures **K1**, **K2** and **K3** (Scheme 7).

In Fig. 2, the spectrum "0 min" shows an additional signal at $\delta \sim 13.51$ ppm which was also detected in the 1/1 charge. We assign this signal to the first transalkylidenation product, presumably the intermediate anti rotamer of **K1** (see Scheme 8). This would correspond to literature values for the chemical shifts of alkylidene protons in similar structures [16,17]. This is further indicated by the presence of neophylene (a transalkylidenation product, see also Scheme 3) of which the resonances from the vinyl protons v_t and v_c can be observed as two double doublets around $\delta \sim 5.0$ ppm (i.e., from the earliest stage of the reaction onward).

2.2.3. Species K1

From the earliest recorded spectra (i.e., short reaction time) up to those recorded after several weeks, the dominant resonance in the alkylidene region is a singlet at $\delta \sim 12.58$ ppm. This we assign to the alkylidene proton **A** in structure **K1** in which the O-coordination results in a stable structure, relaxing strain of bond angles and steric demand. Thus, the five-membered MoCCCO-ring would occupy the equatorial plane of the trig-

onal bipyramid, offering a favorable open OMoC angle (see also Scheme 7). The –OCMe(CF$_3$)$_2$ groups would have sufficient space as the O-coordinated heptyloxy chain could fold outwards.

This picture is supported by explanations regarding the mechanism of the interconversion of syn and anti rotamers in such complexes (Scheme 8) [15].

In such an interconversion there is a stabilized intermediate at a 90° rotation angle which uses the d-orbital from the Mo center involved in the π bonding of the imido ligand. Thus, the imido ligand loses the π bond and bends. Normally this arrangement is not favorable with strong electron withdrawing t-butyloxy groups (i.e., –OCMe(CF$_3$)$_2$) [15], but in our case the O-coordination is offering additional electron density at the center as well as the chelating effect.

These explanations are fully consistent with spectroscopic evidence. The –OCMe(CF$_3$)$_2$ groups are obviously interconverting rapidly between equatorial and axial position as they exhibit only one sharp proton resonance Me at $\delta \sim 1.3$ ppm. But they do feel the steric congestion of the heptyloxy chain from the coordinated oxygen; there is a clear NOE between the protons Me and the O-coordinated side chain methylene protons α' and β' at $\delta \sim 4.49$ and 2.34 ppm, respectively. This distinct NOE is absent for the respective methylene protons α and β ($\delta \sim 3.54$ and 1.63 ppm) of the second heptyloxy chain pointing outward (see also Scheme 4). From two observations there is clear indication of the bending of the imido ligand: first, from the first spectra (i.e., short reaction times) onward, a signal is noticed at $\delta \sim 2.8$ ppm that is neither in the pure catalyst spectrum nor in the pure monomer spectrum. Using the unambiguous assignments in Fig. 3, this signal is due to the methyl protons from the aromatic rest Me$_{A,NPh}$ and compares to $\delta \sim 2.3$ ppm in the original
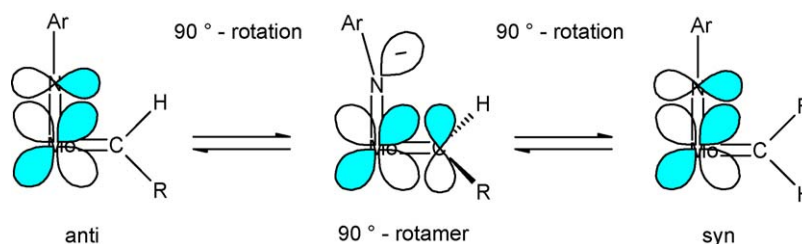
Scheme 8. Interconversion of syn and anti rotamers, from Ref. [15].

catalyst. Second, this bending must not only be strong but the aromatic rest must also be very mobile, as the protons $Me_{A,NPh}$ are only exhibiting one sharp resonance (i.e., there cannot be a preferred orientation because the two methyl groups on the aromat are equivalent). Furthermore, the protons $Me_{A,NPh}$ are experiencing NOEs with protons Me as well as an NOE with the alkylidene proton **A**.

All other data listed in Table 1 are consistent. The determination of coupling proton-carbon pairs helped not only to assign most respective carbon chemical shifts, but also helped to determine which proton signals belonged to which molecule in the proton NMR spectra of the charges.

2.2.4. Species *K2* and *K3*

Due to the small amount of these species in the reaction mixture the determination of relative intensities is less accurate than in the case of **K1**. But the data still are consistent as may be seen from applying the same reasoning regarding the origin of the signals in these cases as was discussed for **K1**. Furthermore, such binuclear complexes are well known from reactions with unsubstituted divinylbenzene [17].

2.2.5. DHepODVB, neophylene and ethylene

The monomer DHepODVB, the transalkylidenation by-product neophylene, and the condensation product ethylene are all present even after more than 3 weeks. Neophylene is released in the transalkylidenation process of the catalyst used (see Scheme 3). The investigated systems were closed systems.

2.2.6. Oligomeric condensation products

The formation of oligomeric condensation products can be followed by the evolution of specific signal groups, such as from the vinylene protons $v_{I,II, etc.}$ around $\delta \sim 7.9$–8 ppm or the methylene protons α of the heptyloxy side groups and others more (see also Scheme 7). The systematic assignment of these products requires an in-depth discussion and is covered elsewhere [10].

2.2.7. Accounting for the product configuration and low reaction rate

The oligomeric condensation products (i.e., the DHepO-PV oligomers) from the ADMET of DHepODVB show *trans* configured vinylene units $v_{I,II, etc.}$ [10]. In order to produce *trans*-vinylene connected products, the styryl units in the molybdenacyclobutane **D** (Scheme 3) must be anti oriented. Scheme 9 illustrates the possible pathways to build up a molybdenacyclobutane with this requirement.

On the left side, two alkylidenes (i.e., possible structures **C** in Scheme 3) are shown. Only the anti rotamer and the 90° rotamer have to be considered. The syn rotamer would not allow any stabilizing O-coordination at the metal center, in addition the long alkyloxy chain would interfere sterically with the imido ligand, thus making this rotamer highly unlikely.

In the case of the anti rotamer, the monomer would have to approach the active site from the upper right quadrants (depicted: rear quadrant), in order to result in an anti orientation in **D**. In the case of the 90° rotamer (e.g., species **K1**), the approach would have to come from the lower right rear
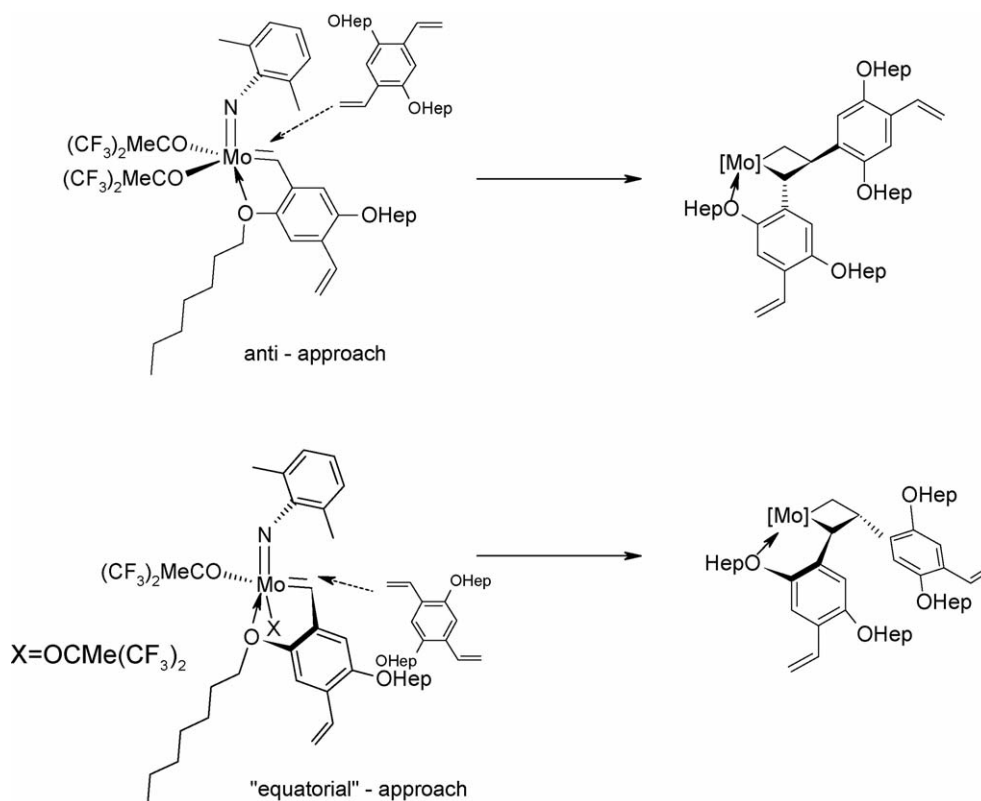
Scheme 9. Possible approach trajectories of DHepODVB toward active alkylidene species.

quadrant, causing strong interaction with at least one alkoxide group.

To explain the dramatically reduced reaction rates of DHep-ODVB compared to DHepDVB (see above), steric arguments will not suffice as both substrates will exhibit steric stress at the active site. Literature reports generally consider syn and anti rotamers of alkylidenes as active species [15]. We offer two possible explanations for the observed behavior.

First, if the anti rotamer is the active species, our system seems to be trapped in the stable 90° rotamer, thus offering no reactive species. In addition, the O-coordination increases steric congestion around the active site, resulting in a drastically reduced probability for the substrate to reach the metal center.

Second, if we assume that the 90° rotamer is a possible reactive species, the steric demand due to the O-coordination is very substantial also, thus inhibiting the approach of new substrate.

In both cases, however, the Mo–O-complexation influences the rearrangements at the metal center that are necessary for the catalytic mechanism. Increasing the reaction temperature increases exchange rates at the metal center thus reduces the stabilization from the O-coordination. Thus the rate of the ADMET-reaction increases.

In this context it is also important to note that replacing the linear heptyloxy chains by branched alkyloxy chains with branching points near the oxygen results in faster ADMET condensations because the O-coordination is hindered, although the overall steric demand of the transition states should be much higher even that in the DHepODVB case [18]. This result gives an additional support that the proven O-coordination is the reason for the hampered metathesis.

3. Conclusion

Novel Mo-alkylidene species containing M–O-complexation were observed and assigned to structures. The slower ADMET condensation of DHepODVB versus DHepDVB could be accounted for. NMR spectroscopical evidence unexpectedly reveals a stabilized alkylidene rotamer (i.e., 90° rotation relative to syn and anti rotamers).

4. Experimental

4.1. Materials and synthesis procedure

All reactions were performed using standard Schlenk techniques, including rigorous exclusion of water and oxygen, and using argon as inert gas. In addition, argon (Linde) was purified by passing it through an adsorber (Oxisorb F, Messer Griesheim). Reaction vessels were annealed by flame under vacuum (Hg diffusion pump).

Toluene-d_8 was stirred 4 h over pure butyllithium, degassed by freeze-pump-thaw cycles and condensed subsequently. The synthesis of 1,4-diheptyloxy-2,5-divinylbenzene is discussed elsewhere [10,18]. The alkylidene complex was synthesized according to literature [19].

4.2. NMR spectroscopy

1D ^{1}H NMR spectra were recorded on a Bruker AC 100 MHz or a Bruker DRX 500 MHz Spectrometer at 25 °C. Two-dimensional (2D) ^{1}H–^{13}C correlation experiments were performed on the Bruker DRX 500 MHz Spectrometer under similar conditions. The following experiments were carried out: COSY, DEPT, HMBC, HMQC and NOE.

Sample concentrations were ~0.5–5 wt% in toluene-d_8 using either solvent or TMS as internal standards or are otherwise specified in the text.

References

[1] Lit. K.J. Ivin, J.C. Mol, Olefin Metathesis and Metathesis Polymerization, Academic Press, San Diego, 1997.
[2] R.H. Grubbs (Ed.), Handbook of Metathesis, three volumes, first ed., Wiley-VCH, Weinheim, 2003.
[3] A. Fuerstner, Angew. Chem. 112 (2000) 3140;
A. Fuerstner, Angew. Chem. Int. Ed. 39 (2000) 3012.
[4] A.H. Hoveyda, R.R. Schrock, Chem. Eur. J. 7 (2001) 945.
[5] R.H. Grubbs, Tetrahedron 60 (2004) 7117.
[6] T.M. Trnka, R.H. Grubbs, Acc. Chem. Res. 34 (2001) 18.
[7] E. Thorn-Csanyi, P. Kraxner, Macromol. Rapid Commun. 16 (1995) 147.
[8] E. Thorn-Csanyi, P. Kraxner, A. Strachota, Macromol. Rapid Commun. 19 (1998) 223.
[9] O. Herzog, O. Narwark, E. Thorn-Csanyi, Synth. Met. 119 (2001) 141.
[10] R. Peetz, A. Strachota, E. Thorn-Csanyi, Macromol. Chem. Phys. 204 (2003) 1439.
[11] E. Thorn-Csanyi, O. Herzog, J. Mol. Catal. A: Chem. 213 (2004) 123.
[12] R. Wehrmann, A. Elschner, E. Thorn-Csanyi, Patent US 6,395,410 B1.
[13] E. Thorn-Csanyi, J.U. Zilles, J. Mol. Catal. A: Chem. 190 (2002) 85.
[14] P. Kraxner, E. Thorn-Csanyi, J. Mol. Catal. A: Chem. 115 (1997) 21.
[15] R.R. Schrock, Tetrahedron 55 (1999) 8141.
[16] R.R. Schrock, H.H. Fox, J.-K. Lee, L.Y. Park, Organometallics 12 (1993) 759.
[17] J.H. Oskam, R.R. Schrock, J. Am. Chem. Soc. 115 (1993) 11831.
[18] R. Peetz, Doctoral Thesis, University of Hamburg, 2000.
[19] R.R. Schrock, J.S. Murdzek, G.C. Bazan, J. Robbins, M. DiMare, M. O'Regan, J. Am. Chem. Soc. 112 (1990) 3875.